View metadata, citation and similar papers at core.ac.uk
brought to you by CORE
provided by UT Digital Repository

Solid Freeform Fabrication 2016: Proceedings of the 27th Annual International Solid Freeform Fabrication Symposium – An Additive Manufacturing Conference
Reviewed Paper

Carbide Formation in Nickel-Base Superalloy MAR-M247 Processed Through Scanning Laser Epitaxy (SLE)

Amrita Basak[1], and Suman Das[1, 2]

[1]George W. Woodruff School of Mechanical Engineering, 813 Ferst Dr NW, Georgia Institute of Technology, Atlanta, GA 30332
[2]School of Materials Science and Engineering, Georgia Institute of Technology, 771 Ferst Dr NW, Atlanta, GA 30313

Abstract

Nickel-base superalloys develop high-temperature strength primarily due to the solid-solution-strengthening and the precipitation-strengthening mechanisms typically through cobalt/chromium and aluminum/titanium respectively. Certain other elements such as boron and zirconium are chosen for grain boundary strengthening. Such elements tend to segregate to the grain boundaries reducing the grain boundary energy and resulting in better grain boundary cohesion and ductility. Another form of grain boundary strengthening is achieved through the addition of carbon and various carbide formers. The carbide formers are responsible for driving precipitation of carbides at grain boundaries and thereby reducing grain boundary sliding. Various types of carbides such as blocky, elongated, and Chinese-script are possible in the microstructures of nickel-base superalloys depending on the composition of the superalloy and processing conditions. However, in the SLE fabricated MAR-M247, only blocky carbides were predominantly observed. Scanning electron microscopy and energy dispersive X-ray spectroscopy investigations were carried out and the carbides were found to be tantalum-rich. This work is sponsored by the ONR through grant N00014-14-1-0658.

Introduction

Nickel-base superalloys are extensively used in aircraft and power-generation turbines, rocket engines, and other challenging high-temperature environments as these alloys offer higher yield strength with increasing operating temperatures primarily due to the presence of the secondary γ′ phases that form an antiphase boundary and lock the associated dislocation movements. For the last few decades, extensive research in superalloy development has culminated in productionization of components with alloys that can withstand temperatures up to 90% of the melting point of the material [1]. However, precipitation of the γ′ phases causes strain age cracking; hardening of the alloy during thermal exposure, and transfer of the solidification strains onto the grain boundaries. The susceptibility to strain age cracking and the alloy weldability is often qualitatively described for nickel-base superalloys by plotting aluminum (Al) vs. titanium (Ti) content in the alloys. The alloy is considered difficult-to-weld if the total Al + Ti content exceeds 4 wt. % [2]. The total Al + Ti content for polycrystalline MAR-M247 is 6.0 wt. %, thus making it a difficult-to-weld alloy.

The degradation of the hot-section components is attributed to creep, thermo-mechanical fatigue, high-temperature oxidation, and thermal corrosion. Currently, the lack of suitable commercial repair technologies results in high maintenance costs for these components that can

reach as much as hundreds of thousands to even millions of dollars per engine. Hence, there is a great commercial interest in developing additive manufacturing (AM) processes that can restore the parent metallurgical microstructure and geometry at damage locations for these parts. Scanning laser epitaxy (SLE) is a metal powder bed fusion-based additive manufacturing process that creates equiaxed (EQ), directionally solidified (DS) and single-crystal (SX) structures in nickel-base superalloys through controlled laser melting of alloy powders onto like chemistry substrates. In SLE, a galvanometer controlled high power laser beam is directed onto the powder bed. Processing parameters such as laser power, scan spacing, and scan speed are varied in SLE to control and optimize the deposit characteristics. An important criterion for a successful SLE deposit is the determination of energy density that ensures a good metallurgical bond between the substrate and the deposit. The metallurgical bond starts at one edge of the substrate where the melt pool is initiated. The melt pool travels along the length of the substrate fusing the powder to the substrate. SLE has been successfully demonstrated to deposit SX CMSX-4 [3-5], EQ René 80 [6] and EQ IN100 [7] on similar chemistry substrates.

MAR-M247 is an equiaxed (EQ) or polycrystalline nickel-base superalloy that was developed at the Martin Marietta Company in the 1970s [8]. Over the last few decades, this alloy has been extensively used in the production of advanced turbine blades and rotating parts in the aerospace industries because of its excellent thermo-mechanical properties. The alloy demonstrates high creep strength and good castability along with excellent oxidation and corrosion resistance at elevated temperatures. MAR-M247 is a nickel-base, vacuum melted, cast superalloy with a high γ' [Ni_3 (Al, Ti)] volume fraction (62%). The alloy also contains a significant amount (13.7 wt. %) of refractory elements such as tantalum (Ta), tungsten (W) and molybdenum (Mo). The semi-coherent γ' phase is the main strengthening phase, which precipitates in the nickel-rich γ matrix. The γ' phase is solid solution strengthened by cobalt, molybdenum, tungsten, and chromium. Carbon (C), boron (B), zirconium (Zr), and hafnium (Hf) precipitate at the grain boundaries primarily in the form of carbides and borides and contribute to improved creep performance. The presence of refractory elements (Ta + W + Mo), the addition of Hf, and the elemental segregation during solidification cause the formation of γ/γ' eutectic and carbides in the interdendritic regions [9-11]. MAR-M247 is commonly used for blade rings and high-pressure turbine blades in gas turbine engines.

The major constituents of the SLE deposited microstructure were the γ matrix, the γ' precipitates in the γ matrix, the eutectics, and the carbides. In the present study, morphologies of the carbide precipitates in the SLE deposited MAR-M247 were characterized. In the SLE deposited MAR-M247, the carbides precipitated in the interdendritic region. The investment cast substrate region revealed the presence of blocky, elongated and Chinese-script carbides. However, in the deposit region, blocky carbides were predominantly present as revealed by the scanning electron microscopy (SEM) investigations. The interface region shows the presence of a few elongated carbides on the deposit side. Energy dispersive X-ray spectroscopy (EDS) measurements revealed that the blocky carbides are mostly Ta-rich. Carbide precipitates near the interface showed trace amounts of boron. Commercially available heat treatment was carried out and the results showed the formation of Cr-rich plate-like discrete carbide network at the grain boundaries. However, the morphologies of the blocky carbides remained unchanged during the heat treatment.

Materials and Methods

Powder of nickel-base superalloy MAR-M247 produced by the Praxair Surface Technologies through Argon gas atomization was used in this study. The composition of the powder is reported in Table I. The morphology and the cross-sections of the powder particles were analyzed using optical microscopy and scanning electron microscopy (SEM). The MAR-M247 powders were mostly spherical, although some irregularity in shape was found as shown in Fig. 1(a). The powder was mounted in Bakelite and polished to a mirror finish. The cross-section was analyzed under an optical microscope for the inspection of internal porosity, and no major internal porosity was detected as shown in Fig. 1(b).

Table I. Chemical composition of the MAR-M247 powder (wt. %)

	Cr	Co	Mo	W	Al	Ti	Ta	Hf	B	C	Zr	Ni
MARM-247	8.0	10.0	0.7	10.0	6.0	1.0	3.0	1.0	0.015	0.15	0.05	Bal

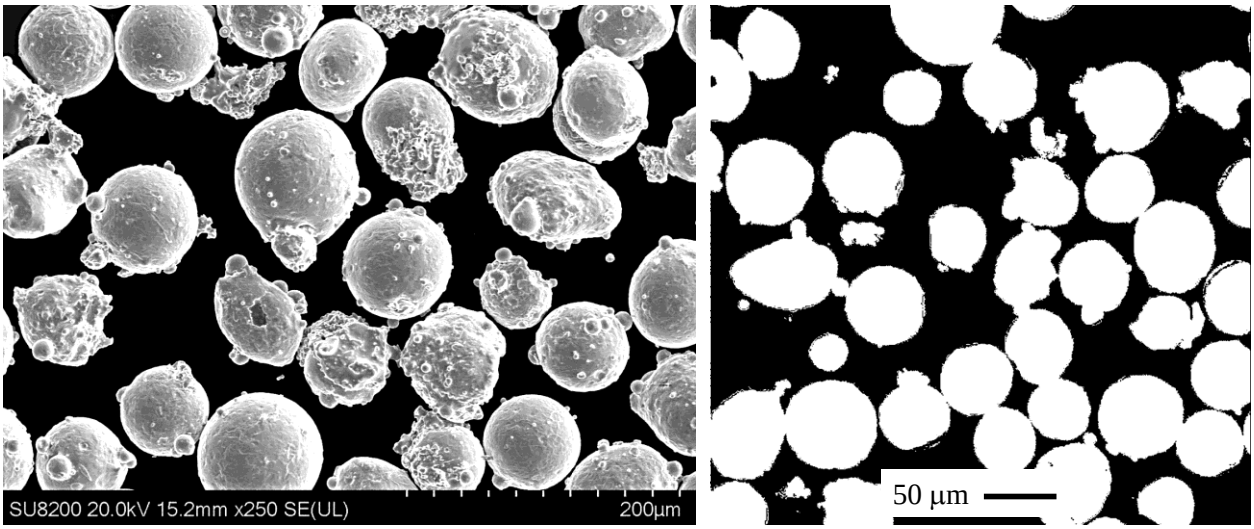

Figure 1. (a) SEM image of the MARM-247 powder, and (b) optical microscopy of the MAR-M247 powder cross-section after polishing.

The SLE process was conducted on rectangular EQ MAR-M247 substrates having dimensions of 31.50 mm x 5.84 mm x 2.54 mm. Each substrate was placed into a 31.50 mm x 5.84 mm recess cut into an IN625 base plate. The MAR-M247 powder was placed above the substrates using rectangular wells cut into an Aluminum mask plate. Once the samples were prepared, they are placed into an atmospheric process chamber that was purged with high purity (99.999%) Argon. A 1kW Ytterbium fiber laser (IPG Photonics, Model: YLS-1000) was used with a Cambridge Technologies galvanometer scanner to focus the beam on top of the substrate to a Gaussian beam diameter of 40 μm. A raster scan pattern across the width of the sample generated

a melt pool that linearly propagated along the length of the substrate. All the samples were run with 25.4 μm scan spacing.

In order to relieve the residual stresses and enable precipitation of the strengthening phases, the samples were heated and kept at 1975 ^{0}F for an hour. Thereafter, the samples were cooled at 10 ^{0}F /minute or faster to a temperature below 1600 ^{0}F. Samples were then given a typical commercial aging treatment consisting of 12 hours at 1600 ^{0}F, followed by air cooling at a minimum average cooling rate of 10 ^{0}F / minute to 1200 ^{0}F to fully develop the strengthening phases.

A Buehler automated saw was used to section the samples for microstructural investigation. Each section was mounted in Bakelite and polished to a mirror finish; starting with 80 grit paper and progressively increasing the size to 1200 grit. The samples were then rough-polished using 5 μm and 3 μm diamond solutions. Finally, the samples were polished using a 0.5 μm colloidal alumina suspension. The polished samples were then etched with Marble's reagent (50 ml HCl, 50 ml H_2O, and 10.0 gm $CuSO_4$) to eliminate the γ' phases revealing the dendritic microstructure. Imaging was then completed using a Leica DM6000 optical microscope. The microstructural investigation of the SLE processed MAR-M247 was carried out on a Hitachi SU8230 SEM.

Results and Discussions

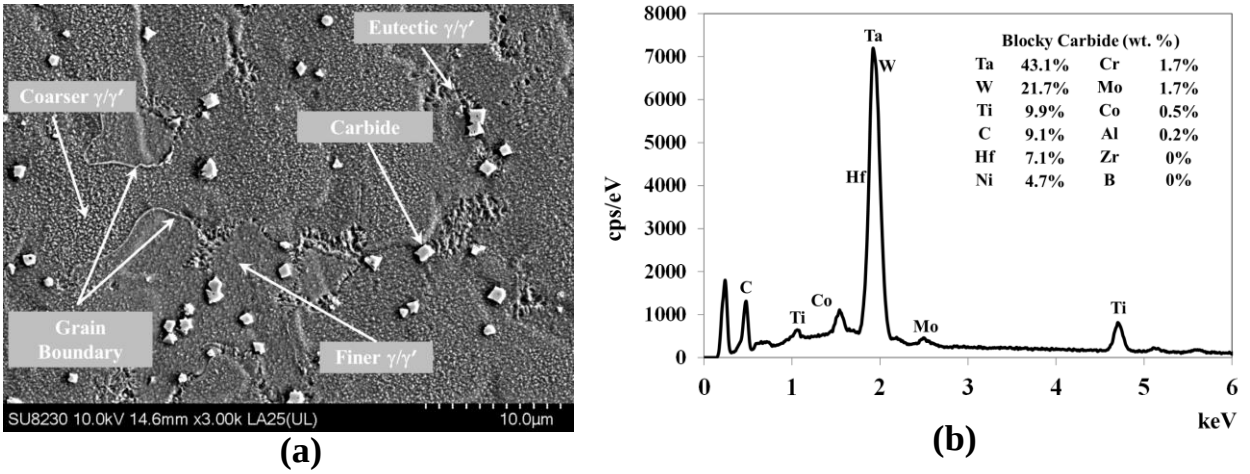

Figure 2. (a) SEM image showing morphologies of various constituents of SLE processed MARM-M247 deposit in the as-deposited sample and (b) SEM-EDS profile of a typical blocky carbide precipitate in the deposit region of the as-deposited sample.

The role of carbides is very complex in nickel-base superalloys. The carbides influence the mechanical properties depending on their morphology and distribution. Fine blocky randomly dispersed carbide precipitates can have strengthening effects on the grain boundaries by inhibiting grain boundary sliding, thus improving creep and rupture strength [12]. On the other hand, if continuous carbide films are formed at the grain boundaries, they might have detrimental effects

on the ductility [12]. Blocky or MC carbides were formed during solidification as discrete particles in the interdendritic regions of the SLE fabricated MAR-M247 as shown in Fig. 2(a). The blocky carbides are very stable at low temperatures but tend to degenerate into secondary carbides at higher temperatures. Figure 2(b) shows the elemental distribution in a typical blocky carbide particle. The carbides were found to be rich in Ta, W, Ti, Hf, and C; however trace amounts of Ni, Cr, Mo, Co, Al, and Cr were also seen to be present. Contrary to the other researchers who reported the presence of Al_2O_3 [13] in the precipitates, in the current study no such aluminum oxide formation is observed primarily due to the trace amount of oxygen present in the processing chamber.

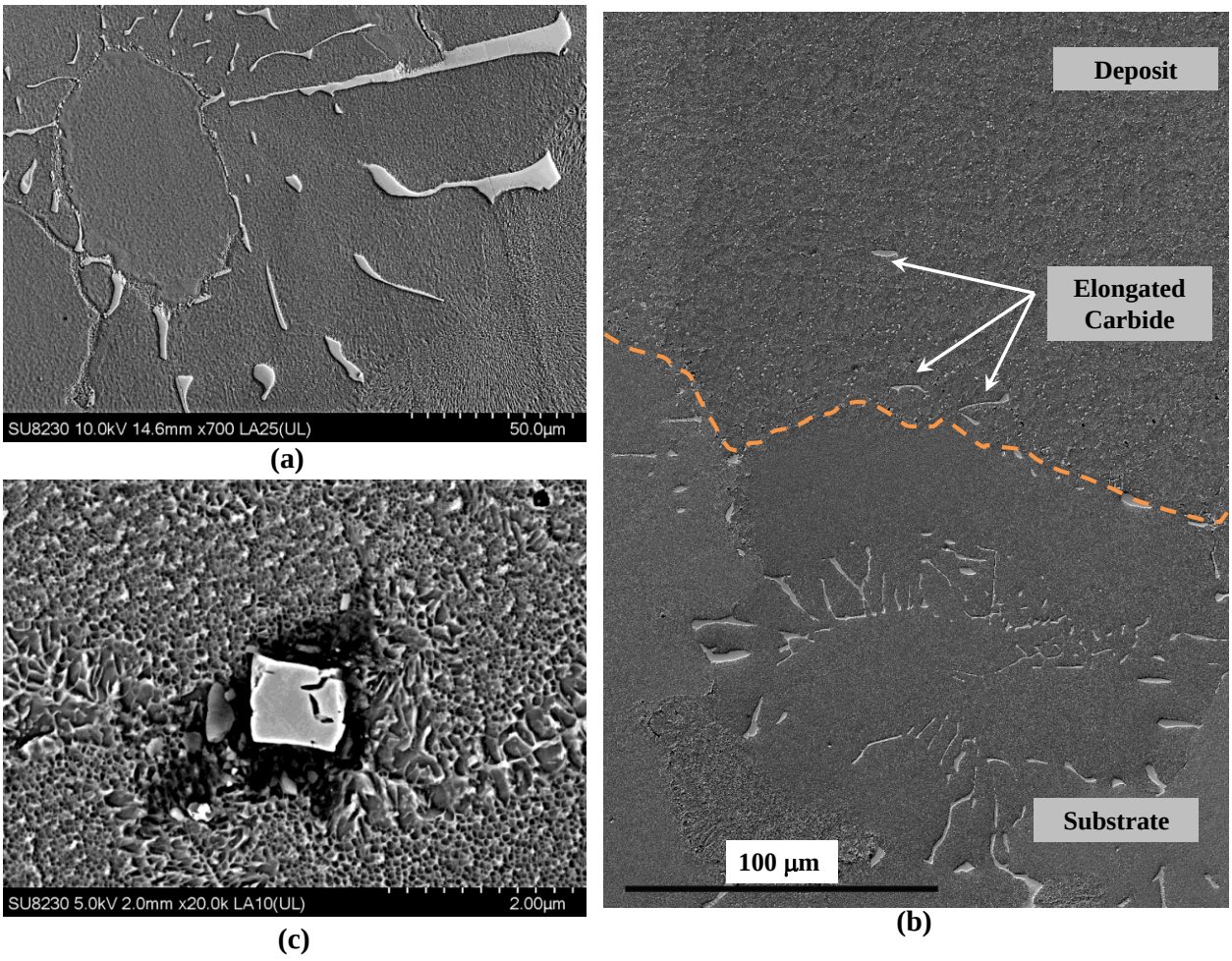

Figure 3. Morphology of the carbide precipitates in the (a) substrate region, and (b) interface region, and (c) deposit region.

Figs. 3(a), 3(b) and 3(c) illustrate the morphology of typical carbide precipitates in the substrate, the interface and the deposit region of the as-deposited sample. The substrate region was abundant with Chinese-script, blocky and elongated carbide precipitates, however in the deposit region, blocky carbides were predominantly observed. However, near the interface, a few elongated carbides were found as shown in Fig. 3(b). This might be due to the fact that during laser processing, a thin layer of the substrate material containing a portion of Chinese-script carbide was

melted. During combined solidification of the partially-melted substrate and the fully melted powder, the existing carbide particles were trapped. Another possible explanation could be convection of the broken Chinese-script carbide arms during laser processing and subsequent solidification of those in the deposit region. The size of the carbide precipitates in the substrate was of order 1-100 μm, while in the deposit the size of the blocky carbides was of order 200-400 nm. Chinese-script carbides typically contain B as reported in the literature [14]. However, B was not observed in any of the blocky carbides that were formed in the deposit region. To verify the hypothesis that the elongated carbides found near the interface were actually from the broken Chinese-script carbides from the substrate region, EDS elemental scan was again performed on the elongated carbides. Figure 4 illustrates the elemental maps for the carbide precipitates near the interface. As can be seen, the elongated carbide precipitate contained only B indicating that the particle was convected from the substrate region.

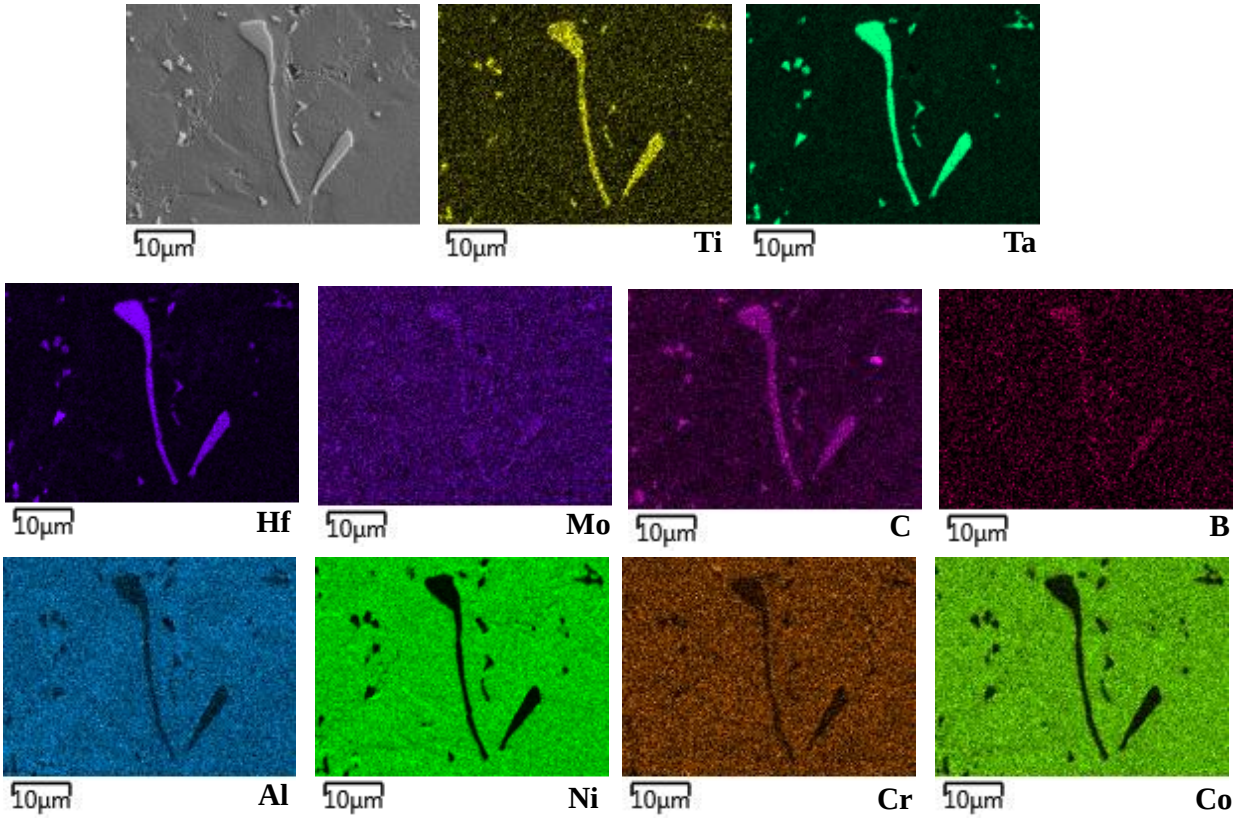

Figure. 4 SEM-EDS elemental maps for various elements in carbide particles deposited near the interface.

Figure 5 reports EDS map of various carbide precipitates in the deposit region of the heat-treated sample. The blocky carbides as mentioned earlier were found to be rich in Ta, W, Ti, Hf, and C; however trace amounts of Mo, Zr, and B were also present. In addition to the blocky or MC type carbides, $M_{23}C_6$ carbides forming discrete thin networks also formed in the heat-treated MAR-M247 samples. $M_{23}C_6$ carbides play a crucial role in the strengthening the alloy by inhibiting the dislocation movements. They usually precipitate at the grain boundaries in Cr-containing alloys

as irregular and discontinuous particles. In the heat-treated MAR-M247 samples, the deposit region showed plate-like carbides that were Cr-rich. Long exposure times at high temperatures resulted in the formation of continuous carbide films along the grain boundaries. Such continuous film formation was shown to affect negatively the ductility and rupture life of the material [12]. In the SLE fabricated MAR-M247, after the heat treatment, only irregular and discontinuous Cr-rich plate-like precipitates were observed.

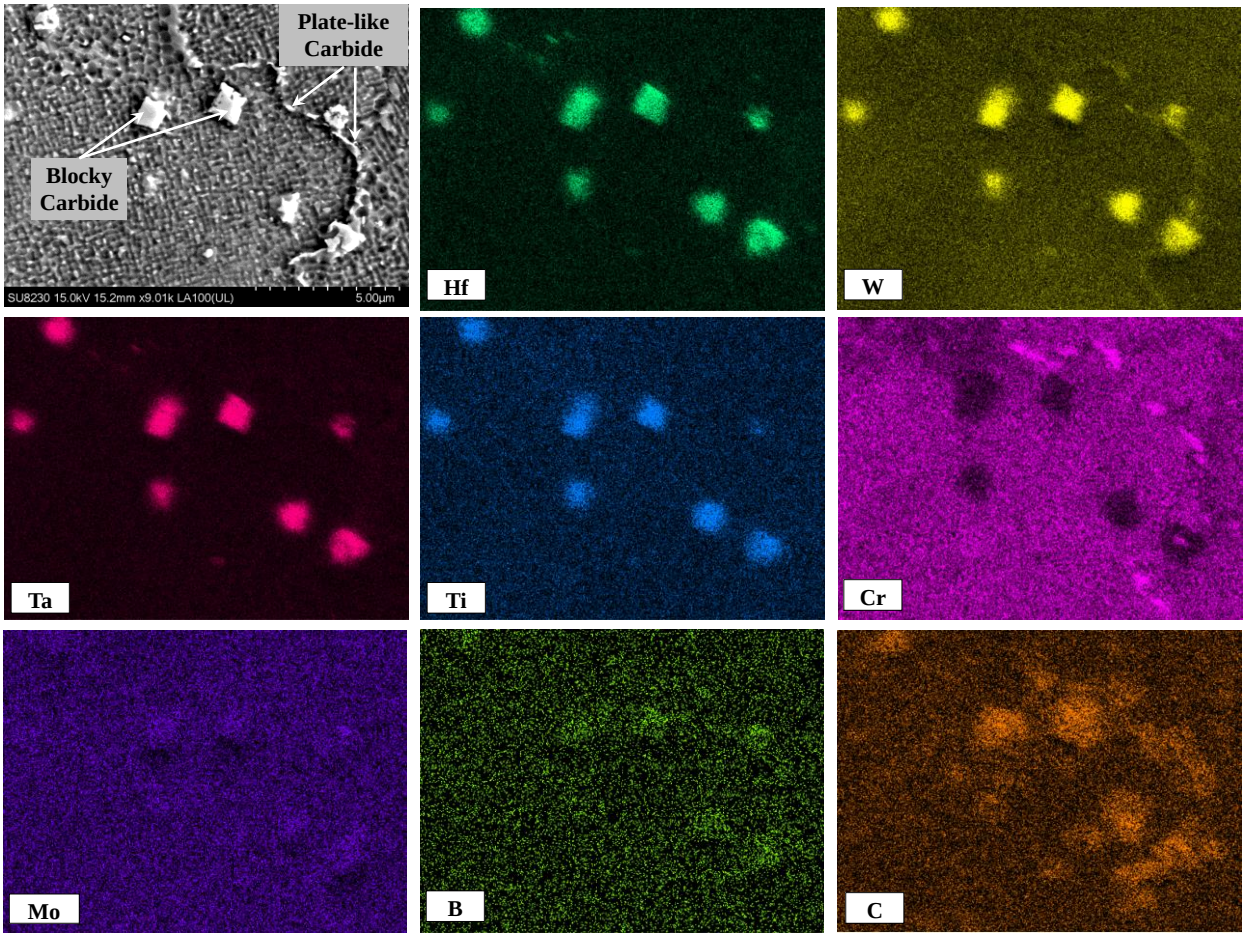

Figure 5. SEM-EDS profile of carbides in the deposit region of a heat-treated sample.

Conclusions

In the present study, SLE deposited MAR-M247 was investigated to characterize carbide formation in the deposited region. MAR-M247 contains about 0.15 wt. % C and 0.015 wt. % B. Minor additions of C resulted in the formation of Ta-rich, MC-type interdendritic primary carbides of predominantly blocky morphologies in the SLE deposited MAR-M247. The blocky carbides were of order 500-1000 nm. Elongated carbides were observed near the interface region. These carbides might be broken pieces of the Chinese-script carbides originated in the substrate region and convected later during combined solidification of the fully melted powder and the partially

melted substrate. The Chinese-script carbides were abundant in the substrate region, however, no such carbide formation was observed in the deposit region. Commercially available heat treatment was carried out, and heat-treated MAR-M247 showed Cr-segregation in the form of a thin plate-like discrete film at the grain boundaries. Further investigation will be carried out in the future to characterize the effect of Cr-rich carbide formation on the ductility of SLE fabricated MAR-M247.

Acknowledgments

This work is sponsored by the Office of Naval Research through grant N00014-14-1-0658.

Disclosures

Dr. Suman Das is a cofounder of DDM Systems, a start-up company commercializing SLE technology. Dr. Das and Georgia Tech are entitled to royalties derived from DDM Systems' sale of products related to the research described in this paper. This study could affect their personal financial status. The terms of this arrangement have been reviewed and approved by Georgia Tech in accordance with its conflict of interest policies.

References

[1] Pollock TM, Tin S. Nickel-based superalloys for advanced turbine engines: chemistry, microstructure and properties. Journal of Propulsion and Power 2006;22:361-74.
[2] Lippold JC, Kiser SD, DuPont JN. Welding metallurgy and weldability of nickel-base alloys: John Wiley & Sons; 2011.
[3] Acharya R, Bansal R, Gambone JJ, Das S. A Coupled Thermal, Fluid Flow, and Solidification Model for the Processing of Single-Crystal Alloy CMSX-4 Through Scanning Laser Epitaxy for Turbine Engine Hot-Section Component Repair (Part I). Metallurgical and Materials Transactions B 2014;45:2247-61.
[4] Acharya R, Bansal R, Gambone JJ, Das S. A Microstructure Evolution Model for the Processing of Single-Crystal Alloy CMSX-4 Through Scanning Laser Epitaxy for Turbine Engine Hot-Section Component Repair (Part II). Metallurgical and Materials Transactions B 2014;45:2279-90.
[5] Basak A, Acharya R, Das S. Additive Manufacturing of Single-Crystal Superalloy CMSX-4 Through Scanning Laser Epitaxy: Computational Modeling, Experimental Process Development, and Process Parameter Optimization. Metallurgical and Materials Transactions A (DOI: 101007/s11661-016-3571-y) 2016.
[6] Acharya R, Bansal R, Gambone JJ, Kaplan MA, Fuchs GE, Rudawski N, et al. Additive Manufacturing and Characterization of René 80 Superalloy Processed Through Scanning Laser Epitaxy for Turbine Engine Hot-Section Component Repair. Advanced Engineering Materials 2015;17:942-50.
[7] Acharya R, Das S. Additive Manufacturing of IN100 Superalloy Through Scanning Laser Epitaxy for Turbine Engine Hot-Section Component Repair: Process Development, Modeling, Microstructural Characterization, and Process Control. Metallurgical and Materials Transactions A 2015;46:3864-75.

[8] Harris K, Erickson G, Schwer R. MAR M 247 Derivations—CM 247 LC DS Alloy, CMSX® Single Crystal Alloys, Properties and Performance. 5th International Symposium on Superalloys 1984. p. 221-30.
[9] Kattus J. Mar-M247 (Code 4218). Aerospace Structural Metals Handbook, Purdue Research Foundation, West Lafayette, Indiana 1999.
[10] Lee H, Lee S. The morphology and formation of gamma prime in nickel-base superalloy. Journal of Materials Science Letters 1990;9:516-7.
[11] Zeisler-Mashl K, Pletka B. Segregation during solidification in the MAR-M 247 system(of nickel-base superalloys). 7th International Symposium on Superalloys 1992:175-84.
[12] Sims C, Stoloff N, Hagel WC. Superalloys II: High Temperature Materials for Aerospace and Industrial Power. 1987. NY: John Wiley & Sons.
[13] Bi G, Sun C-N, Chen H-c, Ng FL, Ma CCK. Microstructure and tensile properties of superalloy IN100 fabricated by micro-laser aided additive manufacturing. Materials & Design 2014;60:401-8.
[14] Basak A, Das S. A Study on the Effects of Substrate Crystallographic Orientation on Microstructural Characteristics of René N5 Processed through Scanning Laser Epitaxy. 13th International Symposium on Superalloys 2016.